Valence Band Studies of Electrochrornic NiO_x Thin Films

M. C. A. Fantini
Instituto de Física, Universidade de São Paulo
C.P. 20516, 01452-990, SP, Brazil

A. Gorenstein
Instituto de Física, Universidade Estadual de Campinas
Caixa Postal 6165, 13081-970 Campinas, S.P., Brazil

K. Subramanian, N. Mainkar, R. L. Stockbauer and R.L. Kurtz
Department of Physics and Astronomy, Louisiana State University
Baton Rouge, LA, 70803-4001, U.S.A.

Received May **13,** 1994

Electrochromic nickel oxide thin films were deposited by RF reactive sputtering, onto glass sibstrates covered with tin dioxide, using different oxygen flux. Variations in the oxygen flux influence the film crystalline structure and stoichiometry, and are related to the electrochromic performance. The films were characterized by cyclic voltammetry, visible spectrophotometry, x-ray diffraction (XRD) and ultraviolet photoemission spectroscopy (UPS). The cyclic voltammetry and visible spectrophotometry results determine the electrochromic performance of the films, in a 0.1 M KOH aqueous electrolyte at different potentials. The XRD data identify the lattice parameter variations due to the (de)- intercalation process and preferred orientation of the films. The UPS results, obtained in a synchrotron radiation facility (CAMD, Baton Rouge, LA, U.S.A.), were used to monitor the valence bands of the films at different coloration states. The film deposited at the smallest oxygen flux (0.5 sccm) is nickel, with a small amount of oxygen, and has a metallic dark appearance. For the next h gher oxygen flux (1.0 sccm) the film is nickel oxide, having a preferred orientation in the (012) direction of the hexagonal cell and a clear as-grown color. For all the other higher fluxes, the material is nickel oxide with (101) preferred orientation and dark. The transmittance span is correlated to the crystalline structure and diffusion coefficient of ions inside the films. The results pointed to modifications in the film composition due to the electrochromic intercalation process. The emergence of bands related to the OH^- concentration in the UPS spectra indicate that the bleached material has a higher number of valence states connected to this radical. On the other hand, the decrease in the occupation of these bands observed for the colored state is followed by an increase in conduction band states over the Fermi eriergy, and account for changes in the optical and electronic properties of the material. Measurements of the UPS spectra at different exciting energies provide the observation of a resonance in the valence band region.

I. Introduction

Non-stoichiometric nickel oxide (NiO_x) thin films, deposited by sputtering, are well known due to their dynamic optical properties[1–3]. The growth of high-performance NiO_x coatings for applications in electrochromic devices depends critically on understanding how the deposition parameters affect the composition, structure and electrochemical behavior. The growth parameters that have to be optimized for the sputtering method are the rf power, the substrate temperature and the oxygen flux. In a previous work we briefly discussed the effect of substrate ternperature on the resulting material properties [3]. In this paper, we present a systematic study of the influence of the

TABLE I. Oxygen flux (f), sample thickness (t) and deposition rate (r).

Sample	f(sccm)	t(A)	r(Å/ sec)
237	0.5	3000	3.3
236	1.0	3150	3.5
233	2.0	2200	1.2
234	4.0	1620	0.68
235	6.0	1900	0.70

oxygen flux on tlie resulting NiO_x deposit. The optical properties of the films were determined by spectrophometry and monochromatic transmittance measurements. The films were also characterized by X-Ray Diffraction (XRD) to determine their structural features, by cyclic voltammetry to evaluate their electrochemical/electrochromic behavior and by Ultraviolet Photoemission Spectroscopy (UPS) to elucidate tlie valence band characteristics at the different coloration states.

II. Experimental

The samples were reactively deposited from a nickel target (99.99%) in an oxygen plus argon atmospliere, under a 7×10^{-3} mbar total pressure, an rf power of 100 W, at room temperature and with target-substrate distance of 150 mm. The films were deposited onto SnO_2/7059 Corning glass substrates (R = 20 Ω/□) using different oxygen fluxes: f = 0.5, 1.0, 2.0, 4.0 and 6.0 sccm. The thickness of the films were determined by a profilometer. Table I depicts the differences on sample deposition conditions, as well as the film thickness.

Tlie electrochemical experiments were conducted in 0.1M KOH aqueous electrolyte, prepared with PA reagents and tri-distilled water. Various galvanostatic steps of 50 μA by 10 min (sample typical area of 1.5 cm^2) were used to evaluate the chemical stabilization of the films. Simultaneously, cyclic voltammetry (-1.0 V vs. SCE and 1.0 V vs. SCE, scanning rate of 20 mV/sec) and transmittance changes were recorded, using a He-Ne laser (λ = 632.8 nm) and a silicon photodetector. The spectral transmittance and total reflectance of the films were measured by a Perkin-Elmer Lambda 9 UV/VIS/NIR spectrophotometer in the range between 350 nm and 850 nm.

The XRD measurements were performed ex-situ on samples submitted to galvanostatic steps of 50 μA for 20 min., using Ni filtered Cu-Kα radiation and step scanning mode, with steps of 0.020° and counting time of 40 sec.

The UPS measurements were performed using the Center for Advanced Microstructures and Devices (CAMD) synchrotron light source. The measurements employed photons in the energy range of 30 - 650 eV delivered by a plane grating monochromator.[4] Angle-integrated spectra were obtained with a display-type analyzer[5] and have been normalized to incident photon flux. The overall resolution was about 1 eV at the highest uv photon energies used here and about 0.25 eV in the photon energy range used to study the Ni 3p resonance. The measurements were performed for one NiO_x sample, grown with tlie highest oxygen flux, f = 6.0 sccm (235 in Table I). This sample was measured in the as-grown, cycled, bleached and colored states, using the same ex-situ conditions employed in the XRD characterization to change tlie optical properties of tlie films.

III. Results

Tlie film deposited at the smallest oxygen flux (0.5 sccm) is mostly nickel, probably with a small amount of oxygen, as determined by the XRD measurements, and has a metallic dark appearance. For the next higher oxygen flux (1.0 sccm) the film is nickel oxide, having a preferred orientation in the (012) direction of the hexagonal cell and a clear as-grown color. For all the otlier higher fluxes, the material is nickel oxide with (101) preferred orientation and dark. Figs. 1 and 2 show diffractograms, corresponding to (101) and (012) reflections. It is remarkable the difference in the crystalline orientation of the film deposited at f = 1.0 sccm when compared to the other obtained samples. Also, Fig. 1 depicts differences in crystalline plane distances among samples at the same optical status, as well as modifications in these distances due to the intercalation/de-intercalation process. Table II presents tlie calculated unit cell values. The NiO_x film deposited with small oxygen flux has a more compressed cell and a smaller variation in unit cell dimensions occurring at the bleaching/coloring procedure. Moreover,

TABLE II Unit cell volume in the as-grown (V_a), bleached (V_b) and colored (V_c) states and percentage difference (V_{bc}).

Sample	$V_a(\text{Å}^3)$	$V_b(\text{Å}^3)$	$V_c(\text{Å}^3)$	$V_{bc}(\text{Å}^3)$
236	55.08	55.21	55.11	0.2
233	57.29	57.54	56.92	1.1
234	56.63	57.43	56.82	1.1
235	57.20	57.35	57.02	0.6
NiO	54.68	–	–	–

$\delta V = 0.37\ \text{Å}^3$ (error in Volume)

for all films the cell dimensions are larger than that of stoichiometric NiO. The calculation of unit cell volumes was based on the determination of diffraction maxima, using a Lorentzian function for the line profile and a straight line background, as it is exemplified in Fig. 3. The changes observed in the lattice parameters (a and c of the hexagonal unit cell) upon de-intercalation, i.e., from bleached to colored state, showed that a always decreased. On the other hand, c increased for the sample deposited with f = 1.0 sccm and decreased for all the other samples, deposited at larger oxygen flux.

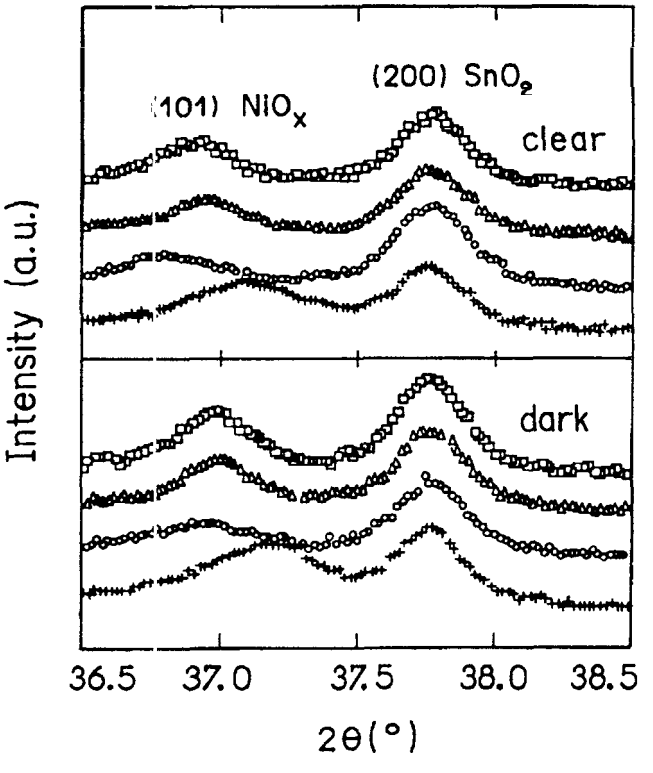

Figure 1: XRD patterns of the samples deposited at f = 1.0 sccm (+), 2.0 sccm (o), 4.0 sccm (A) and 6.0 sccm (□): (101) reflection.

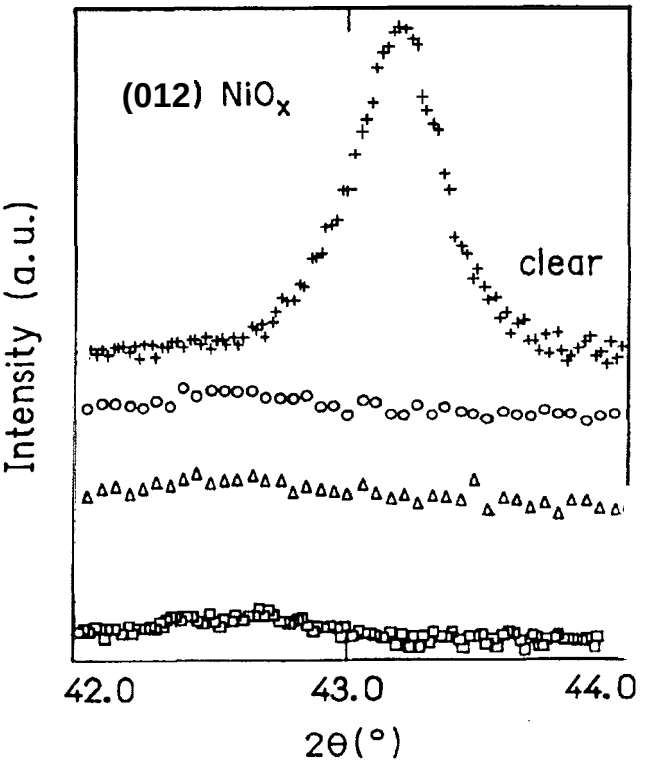

Figure 2. XRD patterns of the samples deposited at f = 1.0 sccm (+), 2.0 sccm (o), 4.0 sccm (A) and 6.0 sccm (□): (012) reflection.

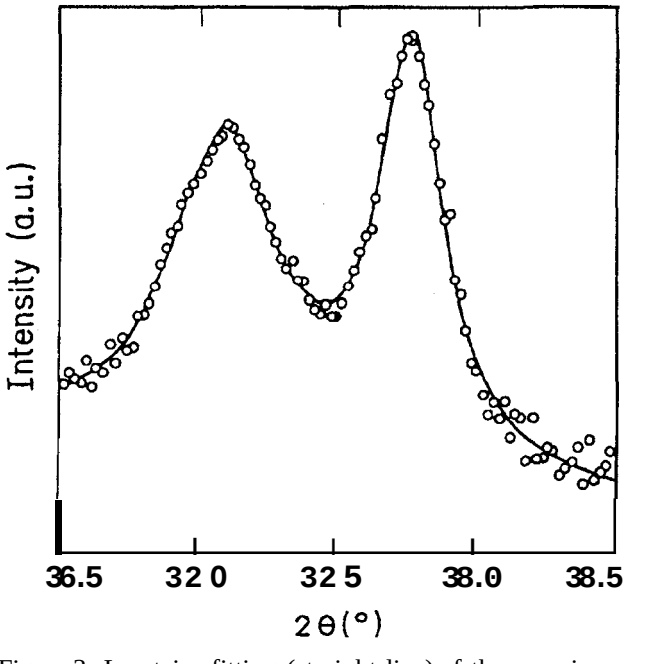

Figure 3. Loretzian fitting (straight line) of the experimental diffracted intensity (open circles) vs. 2Θ for the sample deposited with f = 1.0 sccm in the bleached state. The peak at ~ 37.2' is the (101) NiO reflection and the other at ~37.8° corresponds to the (200) SnO_2 reflection of the substrate.

The analysis of the diffracted integrated intensity provided the preferred orientation of the films, defined as P:

$$P = \frac{I(hkl)}{\sum I(hkl)} .$$

The crystallite size, $D_{(hkl)}$, is obtained from the linewidth[6] with a deviation of ±15 Å. The degree of crystallinity, n, normalized to the larger integrated intensity presented by the 236 sample, is calculated using the total diffractive power of each film.

Table III shows the above mentioned parameters.

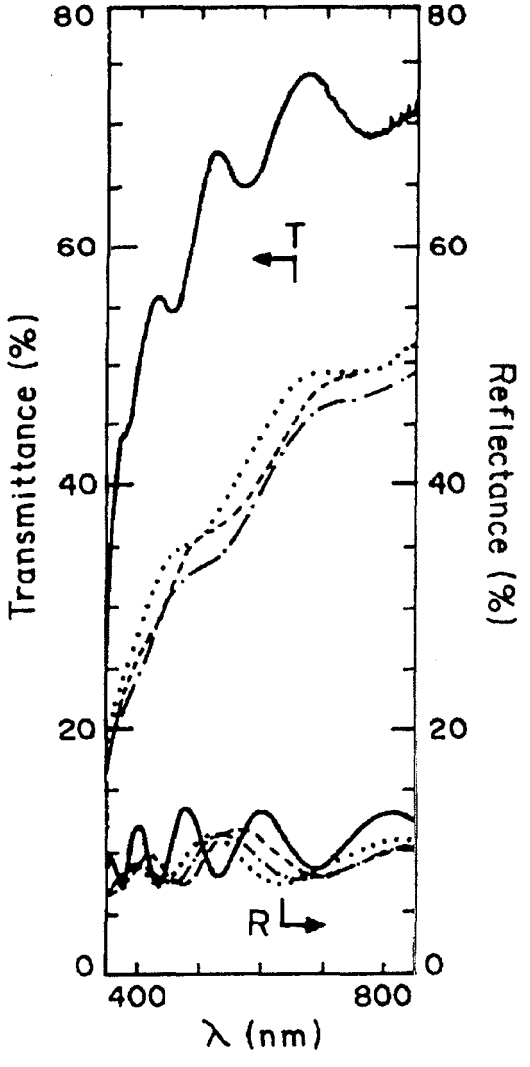

Figure 4. Spectral transrnittance (T) and reflectance (R) of the samples deposited with f = 1.0 sccm (-), 2.0 sccm (- - -), 4.0 sccm (a a •) and 6.0 sccm (– a –).

The results demonstrate quantitatively that the preferred orientation along the (012) direction of the NiO hexagonal cell, achieved with the smaller oxygen flux, gradually changes to a preferred orientation along the (101) crystalline direction as the oxygen flux increases. Nevertlieless, the number of crystallites in this latter direction is always larger than the corresponding number for stoichiometric NiO. Also, tlie crystallite size follows the same trends observed for the preferred orientation, i.e., there is an increase in the crystalline size with the increase of the oxygen flux. The degree of crystallinity, which can be defined as the amount of crystalline phase per unit volume, (n), is larger for the smaller oxygen flux; for larger f-values, the fluctuation of n may be related to deposition rate.

Fig. 4 shows tlie spectral transmittance and total reflectance of the as-grown nickel oxide films in tlie visible region. It is remarkable tlie higher transmittance recorded for the sample deposited with f= 1.0 sccm. The monochromatic transmittance was simultaneously recorded with the cyclic voltammetry. All the samples presented the same variation between minimum and maximum transmittance during the first cycle, around 60%. For the samples deposited with f = 2.0, 4.0 and 6.0 sccm, the results revealed tliat tlie minimum transmittance decreases with cycling, reacliing stabilization at around the 20th cycle. This decrease can reach 60% of the initial value. In tlie mean time, the maximum transmittance also decreases witli cycling, but at a smaller rate. The consequence is a increase in the transmittance span after cycling, around 70%, typically, minimum of 10% and maximum of 80% at the 40th cycle. On the other hand, for the sample deposited at f = 1.0 sccm, the minimum transmittance does not stabilize. The transmittance span attains for the 40th cycle a reasonable value of around 80% (minimum of 16% and maximumof 95%), but both minimum and maximum transmittance values continue decreasing, leading to a variation of only 52% (minimum of 4% and maximum of 56%) after tlie 150th cycle.

Galvanostatic experiments (constant current density) were also performed. In this case, tlie resulting transmittance change for tlie different films is very similar. However, the time variation of the transmittance sliows that the electrochemical process presented by tlie sample deposited at f = 1.0 sccm is much more slower.

TABLE III. Preferred orientation (P), crystallite size (D in Å) and degree of crystallinity (n).

Sample	$P_{(101)}$	$P_{(012)}$	$P_{(110)+(104)}$	$D_{(101)}$	$D_{(012)}$	$D_{(110)+(104)}$	n
236	0.315	0.583	0.102	177	238	106	1.00
233	0.437	0.328	0.235	208	90	164	0.48
234	0.443	0.350	0.233	299	83	165	0.67
235	0.557	0.210	0.233	304	118	168	0.54
NiO	0.261	0.435	0.304	–	–	–	–

The same transmittance span is attained for this sample after a time delay two times greater than those obtained in the experiments performed with the other samples. Fig. 5 shows the cyclic voltammetry and monochromatic transrnittance results obtained for the films after various galvanostatic steps.

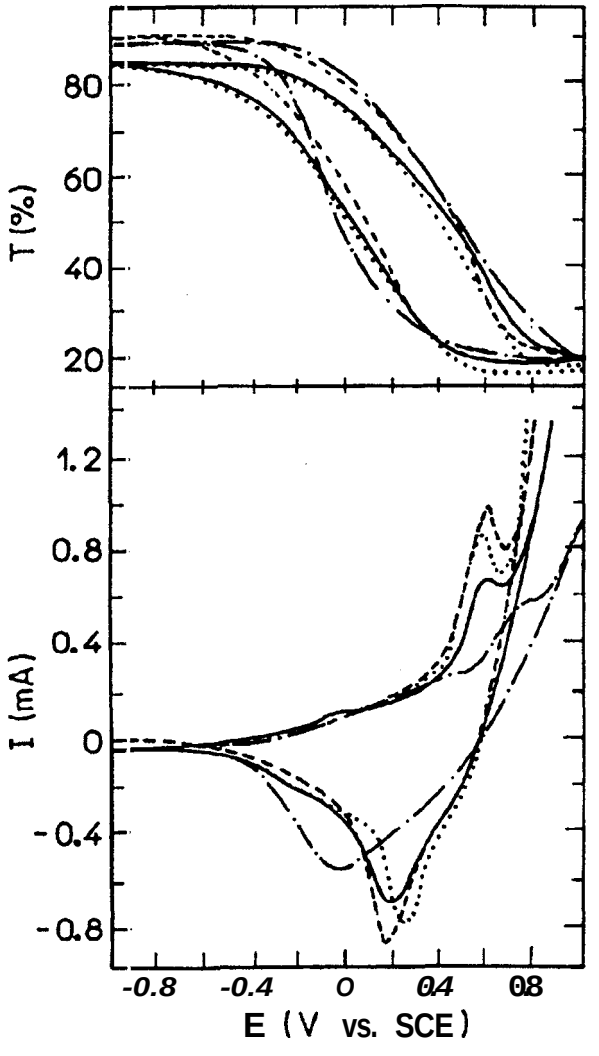

Figure 5. Current (I) and transmittance (T) vs. Potential (E) plots of the samples deposited with f = 1.0 sccm (–r -), 2.0 sccm (-), 4.0 sccm (- - -) and 6.0 sccm (r r r).

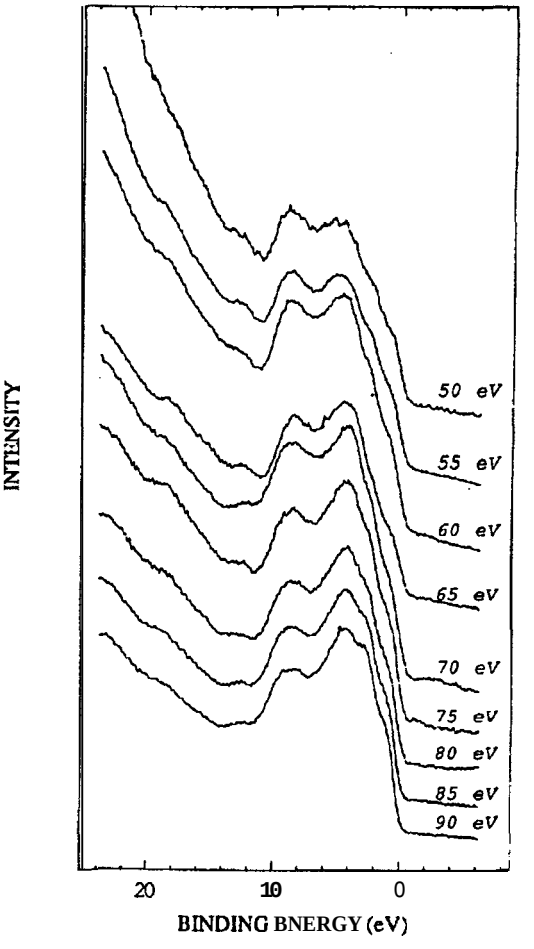

Figure 6. Valence band resonance spectra for different incident photon energies ($h\nu$ in eV).

Fig. 6 shows a typical UPS resonance spectra of the film at the cycled state for different incident photon energies. The differences in peak intensities are due to the Ni-3p threshold resonance at about 66 eV [7]. The whole valence spectrum was described by three Gaussian functions, whose fitting quality is depicted in Fig. 7. The obtained binding energies have been assigned to transitions related to valence band electronic states of pure NiO and NiO with adsorbates[7–10]. Fig. 8 presents the binding energies obtained for the analyzed sample at different coloration states for $h\nu = 70$ eV. Fig.

TABLE **IV.** Binding energy **(B.E.)** and integral intensity (I) obtained from the UPS measurements of 235 sample (f = 6.0 sccm)

Peak ~8 eV				
Samplestatus	as-grown	cycled	bleached	colored
B.E.(eV)	**7.98**	**7.69**	**7.69**	**7.92**
I (10^{-7}a.u.)	**8.01**	**3.23**	**10.2**	**1.38**
I (%)	**35**	**38**	**41**	**35**
Peak ~ **4** eV				
Samplestatus	as-grown	cycled	bleached	colored
B.E.(eV)	**3.31**	**3.31**	**3.79**	**3.97**
I (10^{-7}a.u.)	**13.2**	**4.87**	**12.2**	**1.98**
I (%)	**57**	**57**	**49**	**50**
Peak ~ 1 eV				
Sample status	as-grown	cycled	bleached	colored
B.E. (eV)	**0.39**	**0.56**	**1.38**	**1.19**
I (10^{-7}a.u.)	**1.78**	**0.46**	**2.36**	**0.59**
I(%)	**8**	**5**	**10**	**15**

9 and Table **IV** compile the relevant results concerning, respectively, the integral intensity as a function of photon energy and, for a fixed incident energy, variations in peak position and intensity due to different optical and chemical sample status. The work function of the film at different coloration state did not show any remarkable change, which may be possibly connected to surface coverage of species during electrochemical processing or air exposure. Also, we did not observe any unusual difference in the measured total yield of the films at the whole available photon energy range (30 - 650 eV).

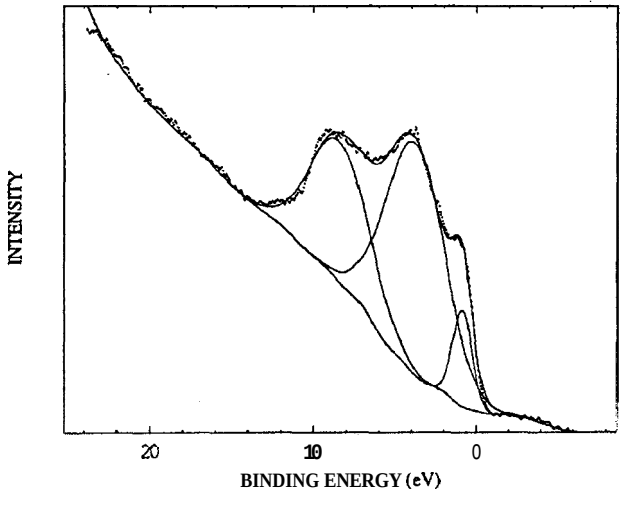

Figure 7. Fitting of valence band spectra by three Gaussian functions.

IV. Discussion

Modifications on the chemical and structural properties of NiO_x thin films, deposited by reactive rf sputtering, are achieved by changing the oxygen flux inside the deposition chamber[11]. These differences can be responsible for variations in the electrochemical/electrochromic performance. First, it is relevant to understand how the oxygen flux affects the material properties and, second, it is important to determine the oxygen flux range that produces NiO_x films with highest electrochromic performance. The parameters to be correlated are stoichiometry, preferred crystalline orientation, crystallite size, degree of crystallinity, transmittance span and electrocliemical stability. In this work we concentrated on the electrochromic, crystalline and optical properties of the different deposited NiO_x thin films.

Due to the fact that the film obtained with f = 0.5 sccm is nickel, instead of nickel oxide, it will not be considered in the further discussion.

The unit cell volume of the sample deposited with f = 1.0 sccm, as well as its variation upon bleaching and coloring is much smaller than the values attained for samples deposited at higher oxygen flux, but the transmittance span after galvanostatic steps is the same for all the different films. On the other hand, other structural parameters like the degree of crystallinity, preferred orientation and crystallite size also depend on the oxygen flux. The film deposited with f = 1.0 sccm presented the highest degree of crystallinity, a larger number of crystallites with the (012) face parallel to the substrate surface and also a larger crystallite size in this same direction, comparatively to the other crystal faces. For higher f values (2.0, 4.0 and 6.0 sccm), the preferred orientation becomes the (101) crystallographic direction and the crystallite size in this direction increases with the oxygen. The observed differences on the crystalline properties can be attributed to the deposition rate, since it is dependent on the oxygen flux, being higher for the smaller values of f.

For f = 1.0 sccm the NiO_x thin film is more transparent in the visible region, even though it is thicker (see Table **I** and Fig. **4).** This result is probably related to stoichiometry[12]. In fact, deviations from

stoichiometry play an important role in the optical, ionic and electronic properties of the materials. In the case of nickrl oxide, the non-stoichiometry has been attributed to excess of oxygen (nickel vacancies) leading to the formation of Ni^{+3} ions in the nickel oxide matrix and to a decrease of transmittance in the visible range[12]. Previous results on the stoichiometry of one similar NiO_x sample grown with f = 2.0 sccm, using Ruthe:ford Back-Scattering measurements, provided $x = .07 \pm 0.02$[13]. It is reasonable to argue that the stoichiometry of the sample deposited at the lowest oxyge:n flux is much near the stoichiometric compound, whicli is transparent in the visible range, than the samples grown with higher flux. However, for this film (f = 1.0 sccm), the monochromatic transmittance do not stabi ize, gradually changing to smaller values under electrochemical cycling. This sample has the slowest time response, indicating a diffusion coefficient lower than for the other samples. Thin film diffusion coefficients are known to greatly depend on the stoichiometry and crystal structure, since the later determines the ionic channels inside the material. In the present case, an ionic transport mechanism linked to the number of oxygen vacancies (hopping ionic transport) should be assumed, since the sample deposited at the lowest oxygen flux is a compound with composition near x = 1, in spite of the greater crystallinity that should nduce a higher diffusion coefficient. As the experimental parameters used in the electrochemical experimerits were the same for all samples, the time scale of the experiment was probably not enough to let the full intercalation/de-intercalation process happen. The optical behavior, then, should be attributed to the slower kinetics of the electrocliemical reaction. Also irreversible incorporation of ionic or neutral species in the oxide matrix should not be discarded. In fact, in earlier works[14,15] we pointed out that alkaline ions also participate in the electrochromic reaction. It is also known that coping of nickel oxide with these ions (A = Li, etc.) originates a dark, p-type semiconductor, $NiO_xA_{(1-x)}$ compound[16]. In order to clarify all these points, work s underway to determine the stoichiometry of the filnis analyzed in this paper.

The fact that the crystal lattice volume is practically the same for the sample deposited with f = 1.0 sccm (Table II) in the as-grown and colored states, even though there is a huge difference in the monochromatic transmittance (70% for as-grown and 16% for colored films), also indicates that either an incomplete intercalation/de-intercalation process or an irreversible incorporation of species occurs for this film. It is important to observe that, independent of the oxygen flux, the obtained films always have crystal lattice parameters larger than the values of stoichiometric NiO and, therefore, the lattice should be able to accept intercalating ions. It has to be pointed out that NiO_x films after electrochemical cycling in aqueous electrolyte do not suffer an hydration process with a consequent amorphization of the crystal structure as has been observed in CoO_x films[17], in spite of similar physical and electrochemical characteristics of NiO_x and CoO_x. All these findings point to the fact that reversibility and large transmittance span, desirable in any electrochromic material, can be achieved in films that combine a proper stoichiometry and structure.

There is not very much information concerning changes in the electronic structure of these non-stoichiometric NiO_x thin films that can be related to electrocliromism, in spite of an extensive literature related to the optical and electronic properties of NiO[12,16,18,19]. Another complication in analyzing, this type of films resides on the fact that the valence band features depend not only on stoichiometry, but also on sarnple crystalline characteristics[20]. The conduction band of these films is frequently explored through the study of the optical properties in the ultra-violet, visible and near-infrared regions, necessary to evaluate the electrochromic performance[1-3]. There are also studies using X-ray Photoemission Spectroscopy (XPS) that focus in modifications in the core levels related to the electrochromic process[2]. Investigations about the valente band of these compounds are scarce, even though important changes upon intercalation/de-intercalation of species are to be expected, since the valence band levels are related to bonding.

The electronic structure of transition metal oxides like NiO has been a controversial subject for a long period of time. The experimental observation that NiO

is a good insulator, instead of a metal as predicted by band theory due to the Ni 3d unfilled band, is the starting point. In the Mott-Hubbard picture tlie controversy was explained by a strong intra-atomic Coulomb interaction between the Ni 3d electrons. In this case the band gap energy is determined by the energy difference (U_{dd}) between Ni d^7 and Ni d^9 configurations. More recently, it was shown that tlie first ionization states are not Ni $3d^7$ but $3d^8\underline{L}$, where $\underline{L}$ is a hole in the O 2p ligand band. In this last case the band gap is a charge transfer gap between ligand holes states and Ni $3d^9$ states. If the charge transfer energy $\mathbf{A} < U_{dd}$ the gap is determined by the charge transfer energy and the width of the ligand band; this is the case predicted for NiO[8,21,22]. The presence of holes induced by doping with acceptors or non-stoichiometry have also been addressed[19,22]

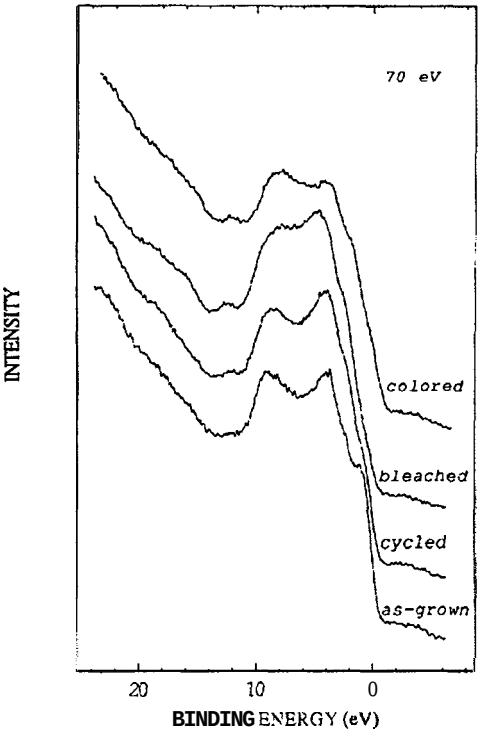

Figure 8. UPS data for the 235 sample at different coloration state, measured with an incident photon energy hv = 70 eV.

The electronic properties of electrochromic nickel oxide thin films were also analyzed in previous works[2,3,11], whose common conclusion is the existence of nickel vacancies in the material giving rise to a p-type semiconductor. The observed extra energy levels are compatible with tlie compound Ni_3O_4 [11]. Another interesting finding, not well understood, is the insensitivity of the Ni 2p core levels to the coloration/bleaching process, while the O 2s levels are modified[2]. Another observation is the appearance of an indirect band gap transition, that is affected by the intercalation process, but not in an extent to justify the huge optical changes observed during the lectrochemical/electrochromic process. On the other hand, the direct band gap is almost insensitive to the same process[3]. This type of correlation between optical and electronic behavior is reasonable if a charge transfer mechanism througli impurity levels separated by small energy gaps is assumed. Dielectric characterization of similar films also points towards this qualitative analysis of electrochromic NiO_x band structure[23].

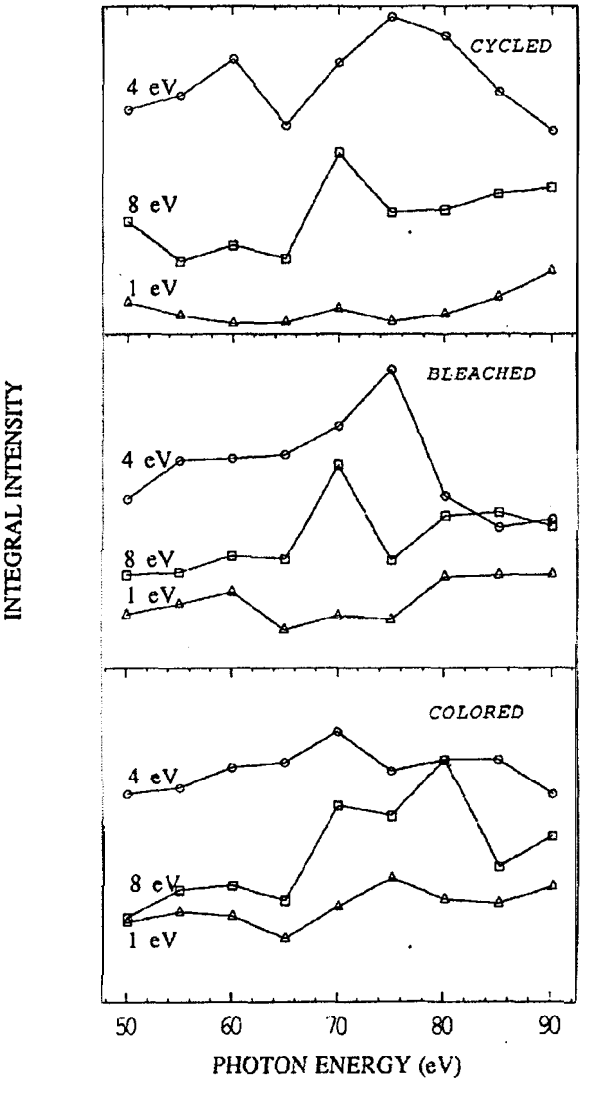

Figure 9. Integral intensity of the three valence band structures as a function of the incident photon energy.

The valence band spectra obtained at the various incident photon energies (Fig. 6) clearly demonstrate the resonance effect promoted by the Ni 3p electrons. The quantitative analysis of this effect is shown in Fig. 9, where it is observed an increase in the integral intensity for $h\nu > 65$ eV, not only in the peaks assigned to Ni 3d levels, but also in those related to O 2p and adsorbed OH^-. The band feature at around 1 eV, associated to Ni 3d levels, showed a larger resonance effect in the colored film. We expect a stronger influence of the nickel in the spectra of dark NiO_x, due to de-intercalation of species that are responsible for charge compensation at the nickel vacancies and changes in the electron and hole conductivity. The most interesting findings of the UPS measurements appear comparing the results obtained for the sample at different coloration states (Fig. 8 and Table IV). Since the as-grown film is opaque and the cycled sample is much more transparent (cycled, stopping at the bleached state), we would expect similarities in the valence band of cycled and bleached samples, as well as in the as-grown and colored ones. Nevertheless, the valence band features of as-grown and cycled films are in some extent similar, since there is a well defined valley between the peaks centered around 4 eV and 8 eV. On the other hand, the samples after electrochemical processing (bleached and colored) present a more smeared band structure, that can be related to freshly adsorbed species on the surface. In fact, the small band observed at around 12 eV in the electrochemical treated films can be associated to OH^- [10]. The energy of the peak centered around 8 eV is equal for the cycled and bleached films and very similar for the other two samples. Moreover, the larger relative intensity of the structure at 8 eV, observed by in the bleached film, is consistent with the fact that it is associated to the OH^- radicals, which are expected to be present in a larger concentration in the bleached film, than in the colored one[15]. The decrease in the intensity contribution of the structure around 4 eV, related to Ni 3d and O 2p levels, can also be explained by the adsorption of species during electrochemical processing. The relative intensity of the peak associated to Ni 3d levels ($\sim$ 1 eV) is higher for the film in the as-grown state when compared to the cycled one. This result can be explained by a decrease in the number of holes originated by nickel vacancies, caused by electrochemical charge compensation in the bleached state. The comparison between bleached and colored films spectra reveals the existence of levels crossing the Fermi energy, forming a type of conduction band in the colored film. In this case the formation of many levels inside the gap, separated by small charge transfer energies, can explain the modification in optical and electronic properties of NiO_x electrochromic material in the bleached and colored states. This band model is consistent with a charge transfer mechanism of hopping carriers across impurity levels and is also compatible with previous experimental data[3,23].

V. Conclusion

Differences in electrochemical/electrochromic performance and structural properties of NiO_x films originated from the variation of oxygen flux during the reactive rf sputtering growth process were analyzed. There is a limitation to deposit NiO_x electrochromic thin films: for f < 0.5 sccm the deposited material is nickel. NiO_x films were obtained for higher oxygen flux (f > 1.0 sccm). The deposition rate is dependent on the oxygen flux, being higher for the smaller values of f. The transmittance span of the films after a number of galvanostatic steps is the same, regardless differences in the structural and optical properties of the as-grown films, but electrocliemical stable films only can be achieved for higher flux of oxygen (f > 2 sccm). The valence band structure modifications observed for the films at different coloration states points to a model of charge transfer mechanism created and destroyed by narrow impurity levels.

Acknowledgments

We thank Mr. A. Lourenço for sample preparation and to Ms. P. S. P. Cardona and Mr. F. F. Ferreira for help in the XRD measurements.

References

1. Large Area Chromogenics: *Materials* and Devices *for Transmittance* Control, edited by C. M. Lampert and C.G. Granqvist, (SPIE Proceedings Series, Bellingham, 1991).

2. A. M. Anderson, W. Estrada, C. G. Granqvist, A. Gorenstein and F. Decker, in *Optical Material Technology for Energy Efficiency and Solar Energy Conversion* IX, edited by C. M. Lampert and C. G, Granqvist, (SPIE Proceedings Series, Bellingham, 1990) vol. 1272, p. 96.
3. M. C. A. Fantini, A. Gorenstein, W. M. Shen and M. Tomkiewicz, in *Optical Materials Technology for Energy Efficiency and Solar Energy Conversion* XI, edited by A. Hugot-Le Goff, C. M. Lampert and C.G. Granqvist, (SPIE Proceedings Series, Bellingham, 1992), vol.1728, p. 41.
4. "Preliminary Performance and Experiments from the High-Resolution Plane-Grating Monochromator at CAMD" Z. Qu, K. Subramanian, N. Mainkar, R. Kurtz, R. Stockbauer, A. Mihill and V. Saile, Nucl. Instrum. and Methods in Phys. Res. A (in press).
5. R. L. Kurtz, S. W. Robey, L. T. Hudson, R. V. Smiglys, and R. L. Stockbauer, Nucl. Instrum. Methods A319, 257 (1992).
6. H. P. Klug and L. E. Alexander, in *X-Ray Diffraction Procedures for Polycrystalline and Amorphous Materials* (Wiley, New York, 1974), 2nd. edition.
7. M. R. Thuler, R. L. Benbow and Z. Hurych, Phys. Rev. B 27, 2082 (1983).
8. G. A. Sawatzky and J. W. Allen, Phys. Rev. Lett. 53, 2339 (1984).
9. J. M. McKay and V. E. Henrich, Phys. Rev. Lett. 53, 2343 (1984).
10. J. M. McKay and V. E. Henrich, Phys. Rev. B 32, 6764 (1985).
11. K. M. E. Miedzinska, B. R. Hollebone and J. G. Cook, J. Phys. Chem. Sol., 49, 1355 (1988).
12. R. Newman and R.M. Chrenko, Phys. Rev., 114, 1507 (1959).
13. J. V. Martins, M. H. Tabacniks, M. C. A. Fantini and A. Gorenstein, Proc. Intern. Workshop on Surf. Eng., Rio de Janeiro (1993), p.42.
14. I. C. Faria, R. M. Torresi and A. Gorenstein, Electrochimica Acta, 38, 2765 (1993).
15. M. C. A. Fantini, I. C. Faria, R. M. Torresi and A. Gorenstein, Proc. 184th Meeting of the Electrochem. Soc., New Orleans, (1993), p. 131.
16. D. Adler and J. Feinleib, Phys. Rev. B 2, 3112 (1970).
17. W. Estrada, M. C. A. Fantini, S. C. Castro, C. M. P. Fonseca and A. Gorenstein, J. Appl. Phys. 74, 5835 (1993).
18. J. L. McNatt, Phys. Rev. Lett. 23, 915 (1969).
19. J. van Elp, H. Eskes, P. Kuiper and G. A. Sawatzky, Phys. Rev. B 45, 1612 (1992).
20. M. D. Rechtin and B. L. Averbach, J. Phys. Chem. Solids 36, 893 (1975).
21. J. Zaanen, G. A. Sawatzky and J. W. Allen, Phys. Rev. Lett. 55, 418 (1985).
22. P. Kuiper, Phd Thesis, Rijks-Universiteit, Groningen, (1990).
23. T. Ivi. J. Nilsson and G. A. Niklasson, in *Optical Materials Technology for Energy Efficiency and Solar Energy Conversion* IX, edited by C. M. Lampert and C. G. Granqvist, (SPIE Proceedings Series, Bellingham, 1990), vol. 1272, p. 129.